1-1-1995

Determination of astrophysical parameters from the spherical gravitational wave detector data

Nadja S. Magalhães
Louisiana State University

Warren W. Johnson
Louisiana State University

Carlos Frajuca
Louisiana State University

Odylio D. Aguiar
Instituto Nacional de Pesquisas Espaciais

Recommended Citation

Magalhães, N., Johnson, W., Frajuca, C., & Aguiar, O. (1995). Determination of astrophysical parameters from the spherical gravitational wave detector data. *Monthly Notices of the Royal Astronomical Society, 274* (3), 670-678. https://doi.org/10.1093/mnras/274.3.670

Mon. Not. R. Astron. Soc. **274,** 670–678 (1995)

Determination of astrophysical parameters from the spherical gravitational wave detector data

Nadja S. Magalhães,[1] Warren W. Johnson,[1] Carlos Frajuca[1] and Odylio D. Aguiar[2]
[1] *Department of Physics and Astronomy, Louisiana State University, Baton Rouge, LA 70803-4001, USA*
[2] *Divisão de Astrofísica, Instituto Nacional de Pesquisas Espaciais, C.P. 515, São José dos Campos-SP, 12201-970, Brazil*

Accepted 1994 December 5. Received 1994 October 31; in original form 1994 July 26

ABSTRACT

The response of a spherical resonant-mass gravitational wave antenna can be written in terms of symmetric trace-free tensors. We apply this formalism to determine the direction of an incoming monochromatic wave, the orientation of its polarization ellipse and the wave's two independent amplitudes, using the response amplitudes at five different points on the sphere surface. This formalism also allows us to determine the directions of burst sources.

Key words: radiation mechanisms: nonthermal – instrumentation: detectors – methods: analytical.

1 INTRODUCTION

Gravitational waves are expected to be an important source of astrophysical information. They are radiated whenever matter has a non-null third time derivative of its quadrupole moment; in regions where gravity is relativistic, this emission should be very strong. One of the main factors that makes gravitational wave astronomy so interesting is the fact that electromagnetic waves are easily absorbed and scattered by matter, while gravitational waves pass through it with impunity (Thorne 1987).

There are several gravitational wave detectors in operation, and other projects are being developed (Blair 1991). In recent years, the construction of a resonant-mass gravitational wave detector using a spherical antenna was proposed (Aguiar et al. 1992). Some theoretical studies were made long ago (Forward 1971; Ashby & Dreitlein 1975; Wagoner & Paik 1977), and recently others have been reported (Johnson & Merkowitz 1993; Zhou & Michelson 1995). One prototype is being tested at Louisiana State University (USA), and an array of this kind of detector is being planned for the coming years (Hamilton et al. 1995).

From the astronomical point of view, the spherical antenna has an important characteristic: because it has five degenerate modes, we should be able to determine the five parameters that give all the information about the gravitational wave from the proper examination of the sphere motion. The determination of the direction, the polarization and amplitude of a gravitational wave, from the response amplitudes of five different points on the sphere surface, is called the 'inverse problem'. In this paper we will assume that the sphere surface radial motion is monitored at five different points by non-resonant, ideal transducers. We will then solve the inverse problem assuming that there is no noise present in the system. We expect this approach to be useful for the investigation of the problem in the presence of noise. The solution found coincides with that of an array of bar detectors (Dhurandhar & Tinto 1988) and, as we will see, this coincidence is not casual.

In Section 2, we present the expression for the radial displacement amplitude of a point on the sphere surface, on the wave's frame.

The simultaneous observation of the radial motion of five points on the sphere's surface is analysed in Section 3, so that the inverse problem can be solved in Section 4.

The main results of the work and some concluding remarks are summarized in Section 5.

2 GENERAL EXPRESSION FOR THE DISPLACEMENT AMPLITUDE

In this work, we will use three different frames. One of them is centred at the sphere's centre of mass, with the $\hat{\boldsymbol{e}}_x$ axis directed towards a chosen point P; we will call it the 'detection point frame' and it will have coordinates (x, y, z) or (ϕ, θ, ψ). The second reference frame will be called the 'wave frame', because it is the wave's proper frame; its coordinates will be (x', y', z') or (ϕ', θ', ψ') and the wave is supposed to propagate in the $\hat{\boldsymbol{e}}_{z'}$ direction. The third reference frame will also be located at the sphere's centre of mass, but it will be rotated relative to the detection point frame; we will name it the 'lab frame', and its coordinates will be (X, Y, Z) or (Φ, Θ, Ψ). Figs 1, 2 and 3 illustrate the relative positions of these frames.

We will assume that only the radial component of the antenna surface displacement will be measured. This observable is given by (see Appendix A)

$$\mathscr{R}(t, \boldsymbol{x}') \equiv \hat{\boldsymbol{r}} \cdot \delta \boldsymbol{d},$$

and in the wave frame it becomes

$$\mathscr{R}^{\mathrm{W}}(t, \boldsymbol{x}') = \sum_{m=-2}^{+2} A^{\mathrm{W}}_{2m}(t)\, a_2(R)\, Y_{2m}(\theta', \phi'), \tag{1}$$

where the only non-vanishing $A^{\mathrm{W}}_{2m}(t)$ are $A^{\mathrm{W}}_{22}(t)$ and $A^{\mathrm{W}}_{2,-2}(t)$.

By Fourier transforming (1), we find

$$\tilde{\mathscr{R}}^{\mathrm{W}}(\omega, \boldsymbol{x}') = \sum_{m=-2}^{+2} \tilde{A}^{\mathrm{W}}_{2\mathrm{m}}(\omega, \boldsymbol{x}')\, a_2(R)\, Y_{2\mathrm{m}}(\theta', \phi'), \tag{2}$$

where

$$\tilde{\mathscr{R}}^{\mathrm{W}}(\omega, \boldsymbol{x}') = \int_{-\infty}^{\infty} \mathscr{R}^{\mathrm{W}}(t, \boldsymbol{x}')\, \mathrm{e}^{-\mathrm{i}\omega t}\, \mathrm{d}t, \tag{3}$$

and, from (A2),[1]

$$\tilde{A}^{\mathrm{W}}_{2m}(\omega, \boldsymbol{x}') = -M^{-1} \frac{\omega^2}{\omega_0^2 - \omega^2 + \mathrm{i}\tau_0^{-1}\omega} \sum_{i,j=1}^{3} \times \int_{V_0} \Upsilon^{ij}_{2m}(\boldsymbol{x}) x^j \rho(\boldsymbol{x})\, \mathrm{d}^3x \{\tilde{h}_+(\omega)\, \Re[m_i(\boldsymbol{x}')\, m_j(\boldsymbol{x}')] + \tilde{h}_\times(\omega)\, \Im[m_i(\boldsymbol{x}')\, m_j(\boldsymbol{x}')]\}. \tag{4}$$

As we show in Appendix B, $\tilde{\mathscr{R}}^{\mathrm{W}}$ can be written as the product of two 3×3 matrices:

$$\tilde{\mathscr{R}}^{\mathrm{W}}(\omega, \boldsymbol{x}') = \sum_{j,k=1}^{3} \tilde{\mathbf{W}}^{\mathrm{W}}_{jk}(\omega, \boldsymbol{x}')\, \tilde{\mathbf{D}}^{\mathrm{W}}_{jk}(\omega, \boldsymbol{x}'), \tag{5}$$

where we introduced

$$\tilde{W}^{\mathrm{W}}_{jk}(\omega, \boldsymbol{x}') \equiv \tilde{h}_+(\omega)\, \Re[m_j(\boldsymbol{x}')\, m_k(\boldsymbol{x}')] + \tilde{h}_\times(\omega)\, \Im[m_j(\boldsymbol{x}')\, m_k(\boldsymbol{x}')] \tag{6}$$

and

$$\tilde{D}^{\mathrm{W}}_{ij}(\omega, \boldsymbol{x}') \equiv -Ra_2(R) \frac{\omega^2(\alpha_2 + 3\beta_2)}{\omega_0^2 - \omega^2 + \mathrm{i}\tau_0^{-1}\omega} \sqrt{\frac{8\pi}{15}} \times [\delta_{i1}(\delta_{j1} y_2 - \delta_{j2} y_4) - \delta_{i2}(\delta_{j2} y_2 - \delta_{j1} y_4)] \tag{7}$$

with $\tilde{D}^{\mathrm{W}}_{22} \equiv -\tilde{D}^{\mathrm{W}}_{11}$ and $\tilde{D}^{\mathrm{W}}_{12} \equiv \tilde{D}^{\mathrm{W}}_{21}$, the other $\tilde{D}^{\mathrm{W}}_{jk} = 0$.

Both the matrices $\tilde{\mathbf{W}}^{\mathrm{W}}$ and $\tilde{\mathbf{D}}^{\mathrm{W}}$ are symmetric and trace free. This kind of matrix can be spanned in terms of the basis[2] of constant tensors $\mathscr{Y}^{2m}_{ij}$ ($m = -2, -1, 0, +1, +2$; $i = 1, 2, 3$), where

$$[\mathscr{Y}^{2,2}_{ij}] = \frac{1}{4}\sqrt{\frac{15}{2\pi}} \begin{bmatrix} 1 & \mathrm{i} & 0 \\ \mathrm{i} & -1 & 0 \\ 0 & 0 & 0 \end{bmatrix}; \qquad \mathscr{Y}^{2,-2} = \mathscr{Y}^{2,2*},$$

$$[\mathscr{Y}^{2,1}_{ij}] = -\frac{1}{4}\sqrt{\frac{15}{2\pi}} \begin{bmatrix} 0 & 0 & 1 \\ 0 & 0 & \mathrm{i} \\ 1 & \mathrm{i} & 0 \end{bmatrix}; \qquad \mathscr{Y}^{2,-1} = -\mathscr{Y}^{2,1*}, \tag{8}$$

$$[\mathscr{Y}^{2,0}_{ij}] = \frac{1}{2}\sqrt{\frac{5}{4\pi}} \begin{bmatrix} -1 & 0 & 0 \\ 0 & -1 & 0 \\ 0 & 0 & 2 \end{bmatrix}$$

and

$$\sum_{i,j=1}^{3} \mathscr{Y}^{2m}_{ij} \mathscr{Y}^{2n*}_{ij} = \frac{15}{8\pi} \delta^{mn}. \tag{9}$$

On this basis, we can also span a particularly useful tensor, $T^{(2)}_{ij}$, which is able to rotate the spherical harmonics from one frame to another (see Dhurandhar & Tinto 1988). For instance, if the wave frame is obtained through a rotation $g(\alpha, \beta, \gamma)$ of the detection point frame (see Fig. 1), then the relation between the spherical harmonics in the detection point frame $[Y_{lm'}(\theta, \phi)]$ and the spherical harmonics in the wave frame $[Y_{lm}(\theta', \phi')]$ is given by

$$Y_{lm}(\theta', \phi') = \sum_{m'=-l}^{l} T^{(l)}_{-m,-m'}(\alpha, \beta, \gamma)\, Y_{lm'}(\theta, \phi). \tag{10}$$

The tensors $T^{(l)}_{ij}$ are given by (Gel'fand, Minlos & Shapiro 1963)

$$T^{(l)}_{mn}(\alpha, \beta, \gamma) = \mathrm{e}^{-\mathrm{i}n\alpha} P^{(l)}_{mn}(\cos\beta)\, \mathrm{e}^{-\mathrm{i}m\gamma} \tag{11}$$

where

$$P^{(l)}_{mn}(\mu) = \frac{(-1)^{l-m} \mathrm{i}^{n-m}}{2^l (l-m)!} \sqrt{\frac{(l-m)!(l+n)!}{(l+m)!(l-n)!}} \times (1-\mu)^{(m-n)/2} (1+\mu)^{-(m+n)/2} \frac{\mathrm{d}^{l-n}}{\mathrm{d}\mu^{l-n}} \times [(1-\mu)^{l-m} (1+\mu)^{l+m}], \tag{12}$$

with $-l \le m, n \le l$. The tensors $T^{(2)}_{mn}(\alpha, \beta, \gamma)$, when spanned in the $\mathscr{Y}^{2m}_{ij}$ basis, assume the form

$$T^{(2)}_{2n}(\alpha, \beta, \gamma) = \sqrt{\frac{8\pi}{15}} \sum_{i,j=1}^{3} \mathscr{Y}^{2n*}_{ij} m^i m^j$$

$$T^{(2)}_{-2n}(\alpha, \beta, \gamma) = \sqrt{\frac{8\pi}{15}} \sum_{i,j=1}^{3} \mathscr{Y}^{2n*}_{ij} m^{*i} m^{*j} \tag{13}$$

$$T^{(2)}_{0n}(\alpha, \beta, \gamma) = \sqrt{\frac{4\pi}{5}} \sum_{i,j=1}^{3} \mathscr{Y}^{2n*}_{ij} n^i n^j.$$

In the wave frame $\boldsymbol{m}$ is given by (A4) while $\boldsymbol{n}$ is given by

$$\boldsymbol{n} = \hat{\boldsymbol{e}}_{z'}.$$

In the detector point frame, using the x-convention (Goldstein 1980) for the rotation $g(\alpha, \beta, \gamma)$ of this frame, we have

$$\boldsymbol{n} = (\sin\beta \sin\alpha, -\sin\beta \cos\alpha, \cos\beta) \tag{14}$$

[1] $\Re(x)$ means the real part of x, while $\Im(x)$ means its imaginary part.

[2] In what follows, we use a formalism very close to that used in Dhurandhar & Tinto (1988).

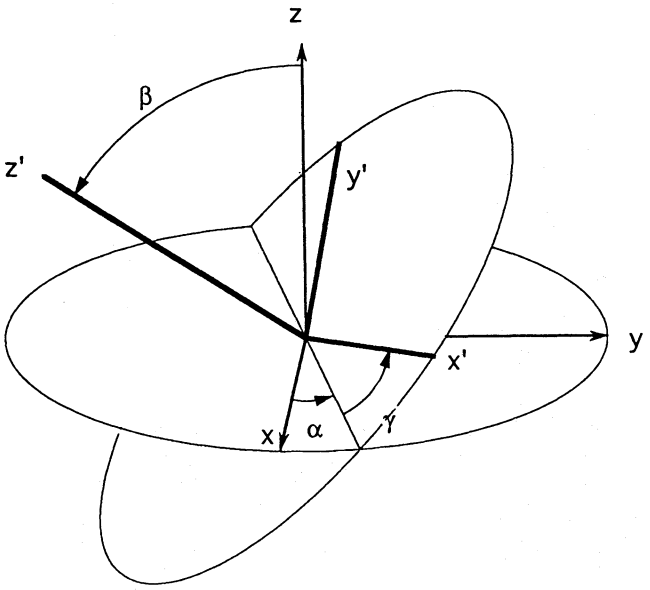

Figure 1. Euler angles between the detection point frame (x, y and z axes) and the wave frame (x', y', and z' axes).

and $\boldsymbol{m}(\alpha, \beta, \gamma) \equiv \boldsymbol{m}_0(\alpha, \beta)\, e^{-i\gamma}$, where

$$\boldsymbol{m}_0(\alpha, \beta) = \frac{1}{\sqrt{2}}(\cos\alpha - i\cos\beta\sin\alpha, \sin\alpha + i\cos\beta\cos\alpha, i\sin\beta). \quad (15)$$

From (9) and (13) it follows that (Dhurandhar & Tinto 1988)

$$\Re(m^i m^j) = \sqrt{\frac{2\pi}{15}} \sum_{n=-2}^{+2} (T^{(2)}_{2n} + T^{(2)}_{-2n})\, \mathcal{Y}^{2n}_{ij}, \quad (16)$$

$$\Im(m^i m^j) = -i\sqrt{\frac{2\pi}{15}} \sum_{n=-2}^{+2} (T^{(2)}_{2n} - T^{(2)}_{-2n})\, \mathcal{Y}^{2n}_{ij}, \quad (17)$$

$$n^i n^j = \sqrt{\frac{16\pi}{45}} \sum_{n=-2}^{+2} T^{(2)}_{0n}\, \mathcal{Y}^{2n}_{ij}. \quad (18)$$

The matrix[3] $\tilde{\mathbf{W}}^{\mathrm{P}}$ can be written in the detection frame using $T^{(2)}_{mn}$ and $\mathcal{Y}^{2m}_{ij}$. Substitution of (16) and (17) in (6) yields

$$\tilde{W}^{\mathrm{P}}_{ij}(\omega, \alpha, \beta, \gamma) = \sqrt{\frac{2\pi}{15}} \sum_{n=-2}^{+2} \mathcal{Y}^{2n}_{ij} \{\tilde{h}_+(\omega)[T^{(2)}_{2n}(\alpha, \beta, \gamma) + T^{(2)}_{-2n}(\alpha, \beta, \gamma)] - i\tilde{h}_\times(\omega)[T^{(2)}_{2n}(\alpha, \beta, \gamma) - T^{(2)}_{-2n}(\alpha, \beta, \gamma)]\}. \quad (19)$$

Because we chose the point P to be located in the direction $\hat{\boldsymbol{e}}_x = (1, 0, 0)$ of the detection point frame, (7) will be written in this frame as

$$\tilde{D}^{\mathrm{P}}_{11}(\omega, \boldsymbol{x}) = -\tilde{D}^{\mathrm{P}}_{22}(\omega, \boldsymbol{x}) = \tilde{\mathscr{C}}(\omega), \qquad \text{other } \tilde{D}^{\mathrm{P}}_{ij}(\omega, \boldsymbol{x}) = 0, \quad (20)$$

[3]The superscript 'P' in $\tilde{\mathbf{W}}^{\mathrm{P}}$ denotes that this function is being described in the detection point frame.

where

$$\tilde{\mathscr{C}}(\omega) \equiv -\frac{Ra_2(R)}{\sqrt{2}} \frac{\omega^2(\alpha_2 + 3\beta_2)}{\omega_0^2 - \omega^2 + i\tau_0^{-1}\omega}. \quad (21)$$

Therefore, using (20) and (19) in (5), we obtain the following expression for the radial motion of the sphere surface at the point P (in the detection point frame):

$$\tilde{\mathscr{R}}^{\mathrm{P}}(\omega, \alpha, \beta, \gamma) = \sum_{m,n=-2}^{+2} \tilde{\mathscr{C}}(\omega)\, \tilde{S}_{mn}(\omega)\, T^{(2)}_{mn}(\alpha, \beta, \gamma), \quad (22)$$

where the only non-vanishing $\tilde{S}_{mn}(\omega)$ are

$$\tilde{S}_{-2,\pm2}(\omega) = \frac{1}{\sqrt{8}}[\tilde{h}_+(\omega) - i\tilde{h}_\times(\omega)],$$
$$\tilde{S}_{+2,\pm2}(\omega) = \frac{1}{\sqrt{8}}[\tilde{h}_+(\omega) + i\tilde{h}_\times(\omega)] \quad (23)$$

and

$$\tilde{S}_{\pm2,0}(\omega) = -\frac{1}{\sqrt{12}}[\tilde{h}_+(\omega) \pm i\tilde{h}_\times(\omega)]. \quad (24)$$

This result is formally the same as that obtained in Dhurandhar & Tinto (1988), for the case of five different bar detectors.

3 OBSERVING THE RADIAL MOTIONS OF FIVE DIFFERENT POINTS ON THE SPHERE SURFACE

In order to evaluate the wave parameters Θ, Φ (the direction of the wave), Ψ (the polarization angle), $\tilde{h}_+$ and $\tilde{h}_\times$ (the amplitudes of the two polarization states), we must have at least five independent measurements of the antenna motion. Therefore we might consider five different points on the spherical detector surface, instead of only one point P. It is convenient to have a common lab frame and five different detection point frames (which depend on the location of the points on the sphere). All the axes are located at the sphere's centre of mass.

If a certain detection point frame is obtained from the lab frame by a rotation[4] $g(\alpha_L, \beta_L, \gamma_L)$ (see Fig. 2), then the response $\tilde{\mathscr{R}}$ of the detector (equation 22) will be given in terms of two sets of Euler angles: (Φ, Θ, Ψ) and $(\alpha_L, \beta_L, \gamma_L)$. An obvious way to write the observable $\tilde{\mathscr{R}}$ in terms of the lab frame coordinates, (Φ, Θ, Ψ), is provided by the addition theorem for $T^{(k)}_{mn}$ (see Gel'fand et al. 1963):

$$T^{(k)}_{mn}(\alpha, \beta, \gamma) = \sum_{s=-2}^{+2} T^{(k)}_{ms}(\Phi, \Theta, \Psi)\, T^{(k)*}_{ns}(\alpha_L, \beta_L, \gamma_L), \quad (25)$$

To write $\tilde{\mathscr{R}}$ in the lab frame coordinates, we need the inverse of the rotation $g(\alpha_L, \beta_L, \gamma_L)$: $T_{g^{-1}} = (T_g)^*$.

Therefore, in terms of the lab frame, the radial displacement of a chosen point on the sphere surface is given by the expression

[4]The index 'L' relates a certain detection point frame with the lab frame. Since we are now considering five different detection point frames, we will allow 'L' to assume the values -2, -1, 0, $+1$ and $+2$.

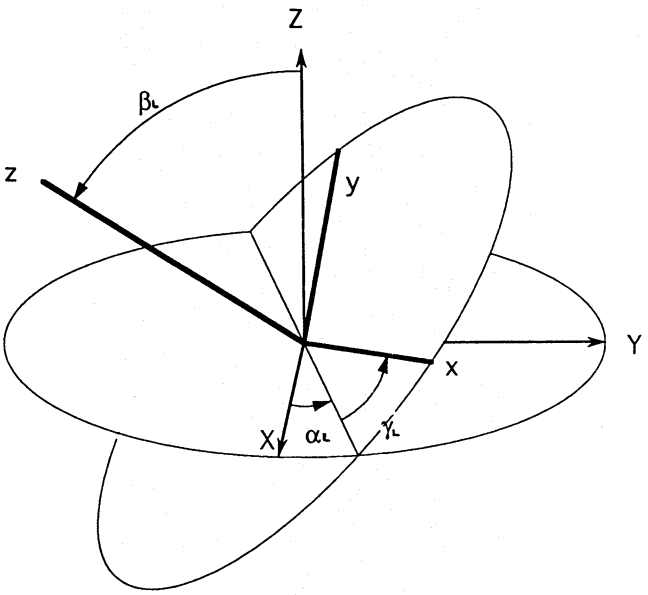

Figure 2. Euler angles between the lab frame (X, Y and Z axes) and the detection point frame (x, y and z axes).

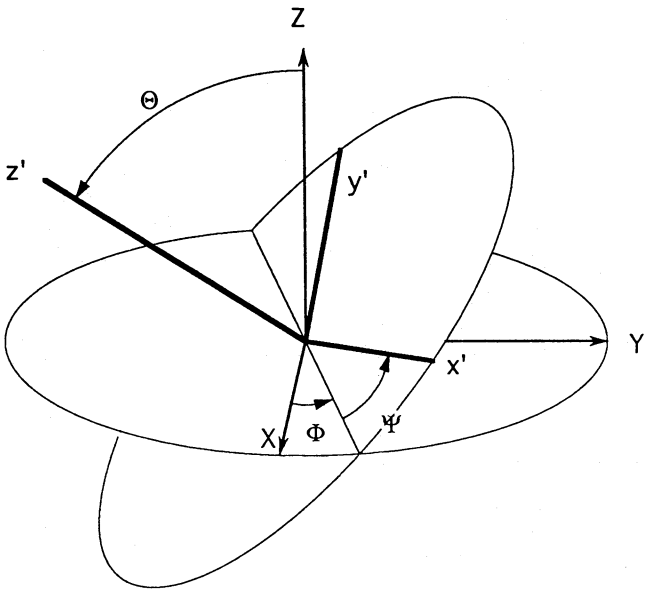

Figure 3. Euler angles between the lab frame (X, Y and Z axes) and the wave frame (x', y', and z' axes).

$$\tilde{\mathcal{R}}^{L}(\omega,\Phi,\Theta,\Psi)=\sum_{m,n,s=-2}^{+2}\tilde{\mathscr{C}}(\omega)\tilde{S}_{mn}(\omega)\times T^{(2)}_{ms}(\Phi,\Theta,\Psi)\,T^{(2)*}_{ns}(\alpha_L,\beta_L,\gamma_L). \tag{26}$$

Because Φ, Θ and Ψ are the angles that describe the wave from the lab's viewpoint, we will define a 5×5 matrix that depends exclusively on the five wave's parameters:

$$\tilde{G}_{sn}[\tilde{h}_\times(\omega),\tilde{h}_+(\omega),\Phi,\Theta,\Psi]\equiv\sum_{m=-2}^{2}\tilde{S}_{mn}[\tilde{h}_\times(\omega),\tilde{h}_+(\omega)]\times T^{(2)}_{ms}(\Phi,\Theta,\Psi). \tag{27}$$

Therefore equation (26) becomes

$$\tilde{\mathcal{R}}_{L}(\omega,\Phi,\Theta,\Psi)=\tilde{\mathscr{C}}(\omega)\,Tr[\tilde{\mathbf{G}}(\omega,\Phi,\Theta,\Psi)\,\boldsymbol{T}^{(2)*}(\alpha_L,\beta_L,\gamma_L)], \tag{28}$$

with $\tilde{\mathscr{C}}(\omega)$ and $\boldsymbol{T}^{(2)*}(\alpha_L,\beta_L,\gamma_L)$ depending exclusively on parameters of the detector.

4 THE INVERSE PROBLEM SOLUTION

We will solve the inverse problem using the same method of Dhurandhar & Tinto (1988). We recall equation (5) in the lab frame coordinates and we expand $\tilde{W}_{jk}$ and $\tilde{D}_{jk}$ on basis (8) as follows:

$$\tilde{W}_{jk}(\omega,\Phi,\Theta,\Psi)=\sum_{s=-2}^{2}\lambda_s(\omega,\Phi,\Theta,\Psi)\,\mathscr{Y}^{2s}_{jk} \tag{29}$$

$$\tilde{D}^{L}_{jk}(\omega)=\sum_{s=-2}^{2}\chi^{L}_{s}(\omega)\,\mathscr{Y}^{2s}_{jk}. \tag{30}$$

The index 'L' goes from -2 to $+2$, labelling the five different points on the sphere's surface. If we use (9) in the above equations, we get

$$\lambda_s(\omega,\Phi,\Theta,\Psi)=\frac{8\pi}{15}\sum_{j,k=1}^{3}\tilde{W}_{jk}(\omega,\Phi,\Theta,\Psi)\,\mathscr{Y}^{2s*}_{jk} \tag{31}$$

and

$$\chi^{L}_{s}(\omega)=\frac{8\pi}{15}\sum_{j,k=1}^{3}\tilde{D}^{L}_{jk}(\omega)\,\mathscr{Y}^{2s*}_{jk}. \tag{32}$$

The χ^{L}_{s} can be calculated and are given by (Dhurandhar & Tinto 1988)

$$\chi^{L}_{s}(\omega)=\sqrt{\frac{2\pi}{15}}\,\tilde{\mathscr{C}}(\omega)\left[T^{(2)}_{2s}(\alpha_L,\beta_L,\gamma_L)+T^{(2)}_{-2s}(\alpha_L,\beta_L,\gamma_L)-\sqrt{\frac{2}{3}}\,T^{(2)}_{0s}(\alpha_L,\beta_L,\gamma_L)\right]. \tag{33}$$

As long as the five $\tilde{D}^{L}_{jk}$ are linearly independent (so that $\boldsymbol{\chi}$ is a non-singular 5×5 matrix), $\boldsymbol{\chi}$ can be inverted so that (30) yields

$$\mathscr{Y}^{2s}_{jk}=\sum_{L=-2}^{2}(\chi^{-1})^{s}_{L}(\omega)\,\tilde{D}^{L}_{jk}(\omega). \tag{34}$$

If we take the complex conjugate of (34), and use (31), we find

$$\lambda_s(\omega,\Phi,\Theta,\Psi)=\frac{8\pi}{15}\sum_{L=-2}^{2}\sum_{j,k=1}^{3}\tilde{W}_{jk}(\omega,\Phi,\Theta,\Psi)\times(\chi^{-1})^{*}_{sL}(\omega)\,\tilde{D}^{L*}_{jk}(\omega). \tag{35}$$

Since $\tilde{D}^{L*}_{jk}(\omega)=[\rho^*(\omega)/\rho(\omega)]\tilde{D}^{L}_{jk}(\omega)$, (35) becomes

$$\lambda_s(\omega,\Phi,\Theta,\Psi)=\frac{8\pi}{15}\frac{\tilde{\mathscr{E}}^*(\omega)}{\tilde{\mathscr{E}}(\omega)}\sum_{L=-2}^{2}\sum_{j,k=1}^{3}(\chi^{-1})^*_{sL}(\omega)\,\tilde{W}_{jk}\times(\omega,\Phi,\Theta,\Psi)\tilde{D}^{L}_{jk}(\omega). \tag{36}$$

From (5), and commutating the operations of conjugation and inversion of the matrix $\boldsymbol{\chi}$, the previous equation can be rewritten as

$$\lambda_s(\omega,\Phi,\Theta,\Psi)=\frac{8\pi}{15}\frac{\tilde{\mathscr{E}}^*(\omega)}{\tilde{\mathscr{E}}(\omega)}\sum_{L=-2}^{2}(\chi^*)^{-1}_{sL}(\omega)\tilde{\mathscr{R}}^{L}(\omega,\Phi,\Theta,\Psi). \tag{37}$$

Finally, (37) and (29) yield

$$\tilde{W}_{jk}(\omega)=\frac{8\pi}{15}\frac{\tilde{\mathscr{E}}^*(\omega)}{\tilde{\mathscr{E}}(\omega)}\sum_{s,L=-2}^{2}(\chi^*)^{-1}_{sL}(\omega)\tilde{\mathscr{R}}^{L}\mathscr{Y}^{2s}_{jk}. \tag{38}$$

Because the spherical antenna is a resonant mass, it will resonate at frequencies from $\omega_0-(2\tau_0)^{-1}$ to $\omega_0+(2\tau_0)^{-1}$, where ω_0 is the central frequency, and τ_0 is the decay time of the energy stored in each of its five fundamental modes. Since we are adopting non-resonant transducers to monitor the sphere surface motions such that the antenna is a free solid, we can rewrite (21) as

$$\tilde{\mathscr{E}}(\Delta\omega)\simeq-\frac{Ra_2(R)}{\sqrt{2}}\frac{Q_0(\alpha_2+3\beta_2)}{2\tau_0\Delta\omega+\mathrm{i}}, \tag{39}$$

where $Q_0\equiv\omega_0\tau_0$ is the mechanical quality factor of the antenna and $\Delta\omega=|\omega_0-\omega|$. The reason for this is that $\Delta\omega\leq(2\tau_0)^{-1}$ and $(Q_0)^{-1}\ll1$, which implies that $(\Delta\omega/\omega_0)\ll1$. In this limit, (38) becomes

$$\tilde{W}_{jk}\simeq\frac{8\pi}{15}\frac{\tilde{\mathscr{E}}^*(\Delta\omega)}{\tilde{\mathscr{E}}(\Delta\omega)}\sum_{s,L=-2}^{2}(\chi^*)^{-1}_{sL}(\Delta\omega)\tilde{\mathscr{R}}^{L}\mathscr{Y}^{2s}_{jk}. \tag{40}$$

Therefore we are able to determine $\tilde{W}_{jk}$ experimentally from (40), as long as we know the detector parameters and the measure of the radial displacements of the sphere surface at five different points ($\tilde{\mathscr{R}}^{L}$). To solve the inverse problem, we have to express $\tilde{W}_{jk}(\omega,\Phi,\Theta,\Psi)$ explicitly in terms of the wave parameters. Dhurandhar & Tinto (1988) have solved a formally identical problem, and found that

$$\tan\Phi=\frac{\tilde{W}_{22}\tilde{W}_{13}-\tilde{W}_{12}\tilde{W}_{23}}{\tilde{W}_{12}\tilde{W}_{13}-\tilde{W}_{11}\tilde{W}_{23}} \tag{41}$$

and

$$\tan\Theta=\pm\frac{\tilde{W}_{12}\tilde{W}_{13}-\tilde{W}_{11}\tilde{W}_{23}}{\tilde{W}^2_{12}-\tilde{W}_{11}\tilde{W}_{22}}\times\left[1+\left(\frac{\tilde{W}_{22}\tilde{W}_{13}-\tilde{W}_{12}\tilde{W}_{23}}{\tilde{W}_{12}\tilde{W}_{13}-\tilde{W}_{11}\tilde{W}_{23}}\right)^2\right]^{1/2}, \tag{42}$$

(which correspond to the two possible locations of the source, diametrically opposed to each other; these results are valid for both bursts and continuous sources). Furthermore,

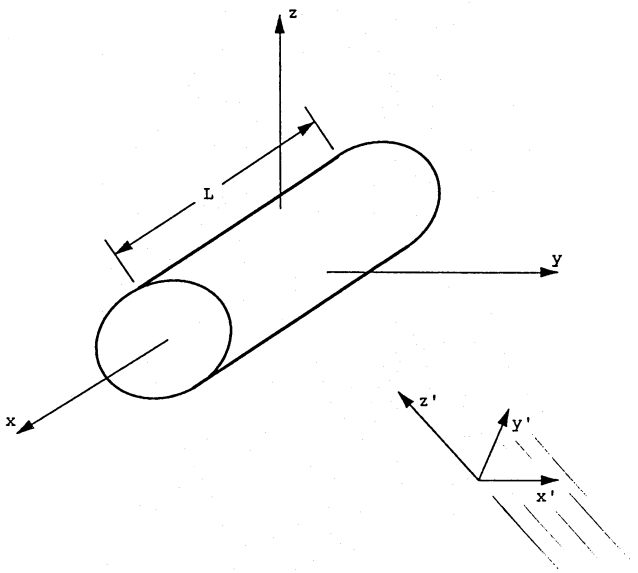

Figure 4. For a cylindrical antenna, the detection point frame (x, y and z axes) coincides with the lab frame. The gravitational wave is assumed to travel in the $\hat{\boldsymbol{e}}_{z'}$ direction of its proper frame (x', y', and z' axes).

for the case that $\tilde{h}_+$ and $\tilde{h}_\times$ are real (as in the case of monochromatic, linearly polarized signals), they obtained[5]

$$\Psi^{\mathrm{M}}=-\frac{\mathrm{i}}{4}\ln\frac{\sum_{i,j=1}^{3}\tilde{W}_{ij}m_{0i}(\Phi,\Theta)m_{0j}(\Phi,\Theta)}{\sum_{i,j=1}^{3}\tilde{W}_{ij}m^*_{0i}(\Phi,\Theta)m^*_{0j}(\Phi,\Theta)}. \tag{43}$$

[(43) has two solutions for Ψ^{M} corresponding to each of the possible solutions for Φ and Θ] and

$$\tilde{h}^{\mathrm{M}}_+=2\sum_{i,j=1}^{3}\tilde{W}_{ij}\Re[m^*_i(\Phi,\Theta,\Psi^{\mathrm{M}})m^*_j(\Phi,\Theta,\Psi^{\mathrm{M}})], \tag{44}$$

$$\tilde{h}^{\mathrm{M}}_\times=2\sum_{i,j=1}^{3}\tilde{W}_{ij}\Im[m^*_i(\Phi,\Theta,\Psi^{\mathrm{M}})m^*_j(\Phi,\Theta,\Psi^{\mathrm{M}})], \tag{45}$$

with $m_i(\Phi,\Theta,\Psi^{\mathrm{M}})$ completely determined from (41), (42) and (43). The possibility of applying Dhurandhar and Tinto's results to the solution of the sphere inverse problem is a consequence of the physical correspondence between an array of bar antennae and the sphere, as we show in Appendix C. This correspondence is possible because we are assuming that there is no noise present in the system (this allows for the degeneracy of the modes) and that the antenna quality factor is high enough to leave the modes uncoupled.

In general, the results (43), (44) and (45) will be valid for any source that emits gravitational waves with polarization amplitudes of the form

$$\tilde{h}_+(\omega)=\tilde{h}_{0+}(\omega)\mathrm{e}^{\mathrm{i}\sigma_+(\omega)}$$

[5]The superscript 'M' in Ψ^{M} indicates that this parameter refers to a monochromatic wave.

and

$\tilde{h}_{\times}(\omega)=\tilde{h}_{0\times}(\omega)e^{i\sigma_{\times}(\omega)}$,

as long as

$\tilde{h}_{0+}(\omega)\sin\sigma_{+}(\omega)=-\tilde{h}_{0\times}(\omega)\sin\sigma_{\times}(\omega)$,

$\tilde{h}_{0+}$ and $\tilde{h}_{0\times}$ being real. This condition assures that $\tilde{h}_{+}(\omega)+\tilde{h}_{\times}(\omega)$ will be real, thus implying a resulting linearly polarized wave.

Equations (44) and (45) may also be used to calculate the polarization amplitudes for burst signals if we arbitrarily choose a value for Ψ (e.g. $\Psi=0$). These results, however, do not provide enough information about the burst polarization unless we somehow increase the bandwidth of observation in such a way as to include most of the burst signal. By either using a multimode resonant antenna or a 'xylophone' of detectors, or both, we are able to determine the burst shape and, therefore, the evolution of the polarization amplitudes with time.

5 CONCLUSIONS

By using a spherical gravitational wave antenna, we were able to determine the five astrophysical parameters of a monochromatic signal: its direction (equations 41 and 42), the polarization angle (equation 43) and the amplitudes of the two polarization states (equations 44 and 45). Possible sources of monochromatic gravitational waves are pulsars or compact binary systems. We were also able to find the direction of astrophysical burst sources of gravitational waves.

In this work, we assumed we were able to monitor the radial motion of a spherical antenna surface at five different points. Besides, we were not concerned about spurious noises at the antenna, and assumed that it had an infinite quality factor; these conditions allow for the complete degeneracy and uncoupling of the modes, so that the antenna response is equivalent to that of an array of cylindrical bars located at the same point in space. The next step should be to include sources of noise in the system, because they are always present in real experiments. Several kinds of noise, such as Brownian noise and back-action of the transducer, can be included by adding random force terms to the right-hand side of (A2). As long as noise, finite quality factor, time resolution of actual measurements and other specific features of a real detection scheme are taken into account in the study of the spherical detector, the similarities between this detector and the bar array will tend to vanish.

An important experimental issue refers to the linear independence among the five points that have to be chosen for the measurements (see equation 34). In the absence of noise this seems to be the case, but it may not happen when the noise is present in the system. Also, the particular distribution of the five points chosen for the measurements may become relevant in the presence of noise.

Finally, the case of a spherical antenna coupled to resonant transducers should also be investigated in future work.

ACKNOWLEDGMENTS

We thank W. O. Hamilton, M. Visco and C. Zhou for helpful comments on the manuscript. CF is supported by a fellowship from CNPq (Brasília, Brazil). NSM acknowledges CAPES (Brasília, Brazil) for financial support. The research by WWJ is supported by NSF under Grant no. PHY-9311731.

REFERENCES

Aguiar O. D. et al., 1992, in Lamberti P. W., Ortiz O. E., eds, Proc. 13th Int. Conf. on General Relativity and Gravitation. Facultád de Mathemática, Astronomía y Física de la Universitad Nacional de Córdoba, Córdoba, p. 455
Ashby N., Dreitlein J., 1975, Phys. Rev., D, 12, 336
Blair D. G., 1991, The Detection of Gravitational Waves. Cambridge Univ. Press, Cambridge
Dhurandhar S. V., Tinto M., 1988, MNRAS, 234, 663
Forward R. L., 1971, Gen. Relativ. Gravitation, 17, 149
Gel'fand I. M., Minlos R. A., Shapiro Z. Ya., 1963, Representations of the Rotation and Lorentz Groups and their Applications. Pergamon Press, New York, p. 87
Goldstein H., 1980, Classical Mechanics, 2nd edn. Addison–Wesley, Reading
Hamilton W. O. et al., 1995, in Proc. 1st Edoardo Amaldi Conference on Gravitational Wave Experiments, in press
Johnson W. W., Merkowitz S. M., 1993, Phys. Rev. Lett., 70, 2367
Merkowitz S. M., Johnson W. W., 1995, Phys. Rev. D, in press
Misner C. W., Thorne K. S., Wheeler J. A., 1973, Gravitation. W. H. Freeman & Co., San Francisco
Thorne K. S., 1987, in Hawking S., Israel W., eds, 300 Years of Gravitation. Cambridge Univ. Press, Cambridge, p. 330
Wagoner R. V., Paik H. J., 1977, in Proc. Int. Symp. on Experimental Gravity. Roma Accademia Nazionale dei Lincei, p. 257
Zhou C. Z., Michelson P. F., 1995, Phys. Rev. D., in press

APPENDIX A: THE SPHERICAL GRAVITATIONAL WAVE ANTENNA MODEL

In this appendix we present the Wagoner & Paik (1977) model for the spherical antenna, which we use for the solution of the inverse problem.

Let $\delta\boldsymbol{d}$ be the displacement of a point P within the spherical gravitational wave antenna relative to its equilibrium position. Because the spherical detector has five eigenmodes $\Upsilon_n(\boldsymbol{x})$, $\delta\boldsymbol{d}$ can be decomposed as

$$\delta\boldsymbol{d}(t,\boldsymbol{x})=\sum_{n=-2}^{2}A_n(t)\Upsilon_n(\boldsymbol{x}). \tag{A1}$$

The complete set of eigenfunctions $\Upsilon_n(\boldsymbol{x})$ is normalized such that

$$\int_{V_0}\Upsilon_n(\boldsymbol{x})\cdot\Upsilon_m^{*}(\boldsymbol{x})\rho(\boldsymbol{x})\,d^3x=\delta_{nm}M,$$

where V_0 is the sphere volume, M is its effective mass and ρ is its density.

Neglecting any sources of noise, and assuming that non-resonant transducers are monitoring the sphere motions, the basic equation governing the response of the detector is (Misner, Thorne & Wheeler 1973)

$$\ddot{A}_n(t)+\tau_0^{-1}\dot{A}_n(t)+\omega_0^2A_n(t)=M^{-1}f_n(t), \tag{A2}$$

where τ_0 is the decay time of the antenna and ω_0 is the frequency of the five degenerate modes.

$f_n(t)$ is the gravitational wave driving force on the detector, given by

$$f_n(t)=\frac{1}{2}\int_{V_0}\sum_{i,j=1}^{3}\Upsilon_n^{i*}(\boldsymbol{x})\,\ddot{h}_{ij}(t)x^j\rho\,\mathrm{d}^3x. \tag{A3}$$

The tensor $h_{ij}(t)$ can also be written in terms of the two polarization states of the gravitational wave, namely '+' and '×' (see Misner et al. 1973). Introducing (Dhurandhar & Tinto 1988) the complex null vector $\boldsymbol{m}$,

$$\boldsymbol{m}\equiv\frac{1}{\sqrt{2}}(\hat{\boldsymbol{e}}_{x'}+\mathrm{i}\hat{\boldsymbol{e}}_{y'}), \tag{A4}$$

where $\hat{\boldsymbol{e}}_{x'}$ and $\hat{\boldsymbol{e}}_{y'}$ are unit vectors in the x', y' directions, respectively, of the wave axes, $h_{ij}(t)$ can be put in the form

$$h_{ij}(t)=2[h_+(t)\Re(m_im_j)+h_\times(t)\Im(m_im_j)]. \tag{A5}$$

Explicitly, in the wave reference frame (assuming the transverse-traceless gauge)

$$h_{x'x'}=-h_{y'y'}=h_+,\qquad h_{x'y'}=h_{y'x'}=h_\times,\qquad \text{all other } h_{ij}=0. \tag{A6}$$

From (A3), $\Upsilon_m(\boldsymbol{x})$ can be put in the form

$$\Upsilon_m(\boldsymbol{x})\equiv\Upsilon_{lm}(\boldsymbol{x})=[a_l(r)\,\hat{\boldsymbol{r}}+b_l(r)\,R\nabla]\,Y_{lm}(\theta,\phi), \tag{A7}$$

where l is even and R is the radius of the sphere. $a_l(r)$ and $b_l(r)$ are dimensionless, real, radial eigenfunctions.

From (A3), (A6) and (A7), it is found that the non-zero components of the driving force[6] $f^{\mathrm{W}}_{lm}(t)$ in the wave-based frame are

$$f^{\mathrm{W}}_{2,2}(t)\equiv f^{\mathrm{W}}_{+}(t)=\sqrt{\frac{4\pi}{15}}\,R(\alpha_2+3\beta_2)\,\ddot{h}_+(t), \tag{A8}$$

$$f^{\mathrm{W}}_{2,-2}(t)\equiv f^{\mathrm{W}}_{\times}(t)=\sqrt{\frac{4\pi}{15}}\,R(\alpha_2+3\beta_2)\,\ddot{h}_\times(t),$$

where

$$\alpha_l\equiv(MR)^{-1}\int_{V_0}a_l(r)\,r^3\rho\,\mathrm{d}r \tag{A9}$$

and

$$\beta_l\equiv M^{-1}\int_{V_0}b_l(r)\,r^2\rho\,\mathrm{d}r. \tag{A10}$$

We will assume that only the radial component of the surface displacement will be measured. This observable quantity is given by

$$\mathscr{R}(t,\boldsymbol{x}')\equiv\hat{\boldsymbol{r}}\cdot\delta\boldsymbol{d},$$

and in the wave frame it becomes

$$\mathscr{R}^{\mathrm{W}}(t,\boldsymbol{x}')=\sum_{l,m=-2}^{+2}A^{\mathrm{W}}_{lm}(t)\,a_2(R)\,Y_{lm}(\theta',\phi'). \tag{A11}$$

[6]The superscript W in $f^{\mathrm{W}}_{lm}(t)$ denotes that the function $f_{lm}(t)$ is being described in the wave frame.

Since we are dealing with gravitational waves, $l=2$. Furthermore, from (A2) and (A8) we can show that the only non-vanishing $A^{\mathrm{W}}_{2m}(t)$ are $A^{\mathrm{W}}_{22}(t)$ and $A^{\mathrm{W}}_{2,-2}(t)$.

APPENDIX B: DETERMINATION OF EQUATION (5)

From (4), we rewrite (2) as

$$\tilde{\mathscr{R}}^{\mathrm{W}}(\omega,\boldsymbol{x}')=\sum_{i,j=1}^{3}\tilde{W}^{\mathrm{W}}_{ij}(\omega,\boldsymbol{x}')\,\tilde{D}^{\mathrm{W}}_{ij}(\omega,\boldsymbol{x}'), \tag{B1}$$

where we defined

$$\tilde{W}^{\mathrm{W}}_{ij}(\omega,\boldsymbol{x}')\equiv\tilde{h}_+(\omega)\Re(m_im_j)+\tilde{h}_\times(\omega)\Im(m_im_j) \tag{B2}$$

and

$$\tilde{D}^{\mathrm{W}}_{ij}(\omega,\boldsymbol{x}')\equiv-\frac{a_2(R)}{M}\,\frac{\omega^2}{\omega_0^2-\omega^2+\mathrm{i}\tau_0^{-1}\omega}\times\sum_{l,m=-2}^{+2}\int_{V_0}\Upsilon^{i*}_{2m}(\boldsymbol{x})x^j\rho(\boldsymbol{x})\,\mathrm{d}^3x\,Y_{2m}(\theta',\phi'). \tag{B3}$$

In order to put (B1) in a more convenient form, we must solve integrals like (see equation B3)

$$I_m=\sum_{i,j=1}^{3}\Re(m_im_j)\int_{V_0}\Upsilon^{i*}_{2m}x^j\rho\,\mathrm{d}^3x. \tag{B4}$$

Substitution of (A7) in (B4) yields

$$I_m=\sum_{i,j=1}^{3}\Re(m_im_j)\int_{V_0}[a_2(r)\,\hat{\boldsymbol{r}}+b_2(r)\,R\nabla]^iY^*_{2m}(\theta,\phi)x^j\rho\,\mathrm{d}^3x. \tag{B5}$$

The relation

$$\frac{1}{2}\Re(m_im_j)x^j=\sum_{j,l=1}^{3}\nabla_i\left[\frac{1}{4}x^l\Re(m_lm_j)x^j\right] \tag{B6}$$

substituted in (B5) implies

$$I_m\equiv I_{1m}+I_{2m}, \tag{B7}$$

where (with $\mathrm{d}\Omega\equiv\sin\theta\,\mathrm{d}\theta\,\mathrm{d}\phi$)

$$I_{1m}\equiv\int a_2(r)\rho r^2\int Y^*_{2m}(\theta,\phi)\,\hat{\boldsymbol{r}}\cdot\nabla\times\left[\frac{1}{2}\sum_{j,l=1}^{3}x^l\Re(m_lm_j)x^j\right]\mathrm{d}\Omega\,\mathrm{d}r \tag{B8}$$

and

$$I_{2m}\equiv R\int b_2(r)r^2\rho\,\mathrm{d}r\int\nabla Y^*_{2m}(\theta,\phi)\cdot\nabla\times\left[\frac{1}{2}\sum_{l,j=1}^{3}x^l\Re(m_lm_j)x^i\right]\mathrm{d}\Omega. \tag{B9}$$

We can separate the spherical harmonics into its real and imaginary parts as follows:

$$Y_{2m}(\theta,\phi)=\frac{\sqrt{2}}{2}\{y_{|m|}(\theta,\phi)+\mathrm{i}[\mathrm{sign}(m)]\,y_{|m|+2}(\theta,\phi)\}, \tag{B10}$$

with

$$\mathrm{sign}(m)\equiv\begin{cases}-1, & m<0,\\ 0, & m=0,\\ +1, & m>0.\end{cases} \tag{B11}$$

The $y_{|m|}$ are called *real spherical harmonics* and obey the following relations

$$\int y_m y_n\,\mathrm{d}\Omega=\delta_{mn}, \tag{B12}$$

$$\int \nabla y_m\cdot\nabla y_n\,\mathrm{d}\Omega=\frac{6}{r^2}\,\delta_{mn}. \tag{B13}$$

Because of the structure of $y_{|m|}(\theta,\phi)$, in the wave frame we can also write (B6) as

$$\nabla_i\left[\sum_{j,l=1}^{3}x^l\Re(m_lm_j)x^j\right]=\nabla_i\left[r^2\sqrt{\frac{8\pi}{15}}\,y_2(\theta,\phi)\right],\qquad i=1,2, \tag{B14}$$

Therefore (B8) becomes

$$I_{1m}=\int a_2(r)r^2\rho\int Y^*_{2m}(\theta,\phi)\,\hat{\boldsymbol{r}}\cdot\nabla(r^2y_2)\,\mathrm{d}\Omega\,\frac{1}{2}\sqrt{\frac{8\pi}{15}}\,\mathrm{d}r \tag{B15}$$

and (B9) becomes

$$I_{2m}=R\int b_2(r)r^2\rho\int\nabla Y^*_{2m}(\theta,\phi)\cdot\nabla(r^2y_2)\,\mathrm{d}\Omega\,\frac{1}{2}\sqrt{\frac{8\pi}{15}}\,\mathrm{d}r, \tag{B16}$$

with $m=-2,-1,0,+1,+2$.

Using (B12) and (B13), we obtain

$$I_{1m}=RM\alpha_2\sqrt{\frac{4\pi}{15}}[\delta_{|m|,2}-\mathrm{i}(\mathrm{sign}\,m)\,\delta_{|m|+2,2}] \tag{B17}$$

and

$$I_{2m}=RM3\beta_2\sqrt{\frac{4\pi}{15}}[\delta_{|m|,2}-\mathrm{i}(\mathrm{sign}\,m)\,\delta_{|m|+2,2}], \tag{B18}$$

where we used the definitions (A9) and (A10).

Therefore (B7) becomes

$$I_n=\sqrt{\frac{4\pi}{15}}MR(\alpha_2+3\beta_2)[\delta_{|n|,2}-\mathrm{i}(\mathrm{sign}\,n)\,\delta_{|n|+2,2}]. \tag{B19}$$

A similar calculation yields

$$\sum_{i,j=1}^{3}\Im(m_im_j)\int_{V_0}[a_2(r)\hat{\boldsymbol{r}}+b_2(r)R\nabla]^iY^*_{2m}(\theta,\phi)\,x^j\rho\,\mathrm{d}^3x$$

$$=\sqrt{\frac{4\pi}{15}}MR(\alpha_2+3\beta_2)[\delta_{|n|,4}-\mathrm{i}(\mathrm{sign}\,n)\,\delta_{|n|+2,4}]. \tag{B20}$$

Rewriting (B1) using (B2), (B3), (B19) and (B20), we get

$$\tilde{\mathscr{R}}^{\mathrm{W}}(\omega,\boldsymbol{x}')=\sum_{j,k=1}^{3}[\tilde{h}_+(\omega)\Re(m_jm_k)+\tilde{h}_\times(\omega)\Im(m_jm_k)]$$

$$\times[-a_2(R)R]\frac{\omega^2}{\omega_0^2-\omega^2+\mathrm{i}\tau_0^{-1}\omega}\sqrt{\frac{8\pi}{15}} \tag{B21}$$

$$\times(\alpha_2+3\beta_2)[\delta_{i1}(\delta_{j1}y_2+\delta_{j2}y_4)-\delta_{i2}(\delta_{j2}y_2-\delta_{j1}y_4)].$$

This expression can again be put in the form (B1) as long as

$$\tilde{D}^{\mathrm{W}}_{ij}(\omega,\boldsymbol{x}')\equiv-Ra_2(R)\frac{(\alpha_2+3\beta_2)\,\omega^2}{\omega_0^2-\omega^2+\mathrm{i}\tau_0^{-1}\omega}\sqrt{\frac{8\pi}{15}} \tag{B22}$$

$$\times[\delta_{i1}(\delta_{j1}y_2+\delta_{j2}y_4)-\delta_{i2}(\delta_{j2}y_2-\delta_{j1}y_4)],$$

with $\tilde{D}^{\mathrm{W}}_{22}\equiv-\tilde{D}^{\mathrm{W}}_{11}$ and $\tilde{D}^{\mathrm{W}}_{12}\equiv\tilde{D}^{\mathrm{W}}_{21}$, the other $\tilde{D}^{\mathrm{W}}_{\mathrm{jk}}\equiv0$. (These choices ensure that the matrix $\tilde{\mathbf{D}}^{\mathrm{W}}$ is symmetric and trace-free.)

APPENDIX C: PHYSICAL RELATIONSHIP BETWEEN AN ARRAY OF BARS AND THE SPHERICAL ANTENNA

When only the gravitational wave is exciting a resonant detector (e.g. a cylindrical bar or a sphere with degenerate, uncoupled modes) the antenna response is given by (A2). For a bar antenna with mass M_{B} the only mode sensitive to gravitational waves in the long, thin bar approximation is given by

$$\Upsilon^{\mathrm{BAR}}(\boldsymbol{x})=\hat{\boldsymbol{e}}_x\sin\frac{\pi x}{L}.$$

L is the bar length (supposed much bigger than the cylinder radius in this approximation) and $\hat{\boldsymbol{e}}_x$ is in the same direction as the cylinder axis (see Fig. 4). From (A3), we find, in this approximation,

$$f^{\mathrm{BAR}}(t)=\frac{M_{\mathrm{B}}}{\pi^2}L\ddot{h}_{xx}(t). \tag{C1}$$

For a spherical antenna with mass M_{S}, the reference frame analogous to the one used in the above calculation is the detection point frame (Fig. 1). Each transducer of the

spherical detector can monitor only the radial motion of a point on the sphere surface located on the $\hat{e}_x$ direction of the respective detection point frame. From this frame viewpoint, the sphere quadrupole zero mode, $\Upsilon_0(x)$, is enough to describe the motion of this point, and the corresponding gravitational wave driving force is proportional to (Merkowitz & Johnson 1995)

$$f_0^{\mathrm{SPHERE}}(t) = M_S R \ddot{h}_{xx}(t), \tag{C2}$$

with $h_{xx}(t) = (\sqrt{3}/2)\, h_+(t) \sin^2\beta$.

Because of the proportionality of (C1) and (C2) we conclude that an array of n cyclical bars will respond to the gravitational wave in a similar way as the non-noisy, high-Q spherical antenna monitored by n transducers.